Chapter II

Experimental Section

2.1. Source and purification of the chemicals used

All the chemicals used in various works embodied in this dissertation were of analytical reagent grade (A. R) and were used without further purification as procured from various commercial sources. The chemicals used are listed in the Table 2.1.

Table 2.1. List and source of chemicals used.

Chemical compound	Mol. Formula	Purity	Source	CAS NO.
Copper nitrate	$Cu(NO_3)_2{\cdot}3H_2O$	98%	S.D. Fine Chemicals, India	10031-43-3
1,10-phenanthroline	$C_{12}H_8N_2$	99%	S.D. Fine Chemicals, India	66-71-7
3,5-Dinitrobenzoic acid	$C_7H_4O_6N_2$	98.5%	S.D. Fine Chemicals, India	99-34-3
Thiosemicarbazide	CH_5N_3S	98%	S.D. Fine Chemicals, India	79-19-6
Pyridine-2-carboxylic acid (Picolinic acid)	$C_6H_5NO_2$	99%	S.D. Fine Chemicals, India	98-98-6
Benzene-1,3,5-tricarboxylic acid (Trimesic acid)	$C_9H_6O_6$	99%	S.D. Fine Chemicals, India	554-95-0
4-hydroxy benzoic acid	$C_7H_6O_3$	99%	S.D. Fine Chemicals, India	99-96-7
1-methyl imidazole	$C_4H_6N_2$	99%	S.D. Fine Chemicals, India	616-47-7
Triethyl amine	$C_6H_{15}N$	99%	Sigma-Aldrich, Germany	121-44-8
Potassium bromide	KBr	99%	Sigma-Aldrich, Germany	7758-02-3
Diethyl ether	$C_4H_{10}O$	99%	Sigma-Aldrich, Germany	60-29-7

Ethanol	C_2H_5OH	99%	Sigma-Aldrich, Germany	64-17-5
Methanol	CH_3OH	99.8%	Sigma-Aldrich, Germany	67-56-1
Benzaldehyde	C_7H_6O	99%	Sigma-Aldrich, Germany	100-52-7
4-methyl benzaldehyde	C_8H_8O	99%	Sigma-Aldrich, Germany	104-87-0
2-methyl benzaldehyde	C_8H_8O	99%	Sigma-Aldrich, Germany	529-20-4
4-methoxy benzaldehyde	$C_8H_8O_2$	98%	Sigma-Aldrich, Germany	123-11-5
2-methoxy benzaldehyde	$C_8H_8O_2$	98%	Sigma-Aldrich, Germany	135-02-4
4-chloro benzaldehyde	C_7H_5OCl	97%	Sigma-Aldrich, Germany	104-88-1
2-chloro benzaldehyde	C_7H_5OCl	99%	Sigma-Aldrich, Germany	88-98-5
4-fluoro benzaldehyde	C_7H_5OF	98%	Sigma-Aldrich, Germany	459-57-4
4-nitro benzaldehyde	$C_7H_5NO_3$	98%	Sigma-Aldrich, Germany	555-16-8
2-nitro benzaldehyde	$C_7H_5NO_3$	98%	Sigma-Aldrich, Germany	552-89-6
3-nitro benzaldehyde	$C_7H_5NO_3$	99%	Sigma-Aldrich, Germany	99-61-6
4-(dimethylamino) benzaldehyde	$C_9H_{11}NO$	98%	Sigma-Aldrich, Germany	100-10-7
4-hydroxy benzaldehyde	$C_7H_6O_2$	98%	Sigma-Aldrich, Germany	123-08-0
2-hydroxy benzaldehyde	$C_7H_6O_2$	98%	Sigma-Aldrich, Germany	90-02-8
4-hydroxy-3-methoxy benzaldehyde	$C_8H_8O_2$	99%	Sigma-Aldrich, Germany	121-33-5

Picolinaldehyde	C_6H_5NO	99%	Sigma-Aldrich, Germany	1121-60-4
Thiophene-2-carbaldehyde	C_5H_4OS	98%	Sigma-Aldrich, Germany	98-03-3
Furan-2-carbaldehyde	$C_5H_4O_2$	97%	Sigma-Aldrich, Germany	498-60-2

2.2. Reaction Autoclave

The growth of single crystals using hydrothermal method is carried out in stainless steel Teflon-lined autoclave. Since the reported compounds were synthesized directly in the reaction vessel, the autoclave should be such that it can sustain corrosive solvents at high pressure and temperature for longer reaction time. Hence, the autoclave must be corrosion resistant and should bear high pressure and temperature for longer span of time. Thus autoclaves used for hydrothermal synthesis must have the following characteristic features:

i) It should be inert to bases, acids and oxidizing agents.

ii) It should be assembled and dissembled easily.

iii) The length of the autoclave should be sufficient enough such that desired temperature gradient can be maintained.

iv) The autoclave must be leak-proof over the range of temperature and pressure.

v) It should be capable of bearing high pressure and temperature for long reaction time.

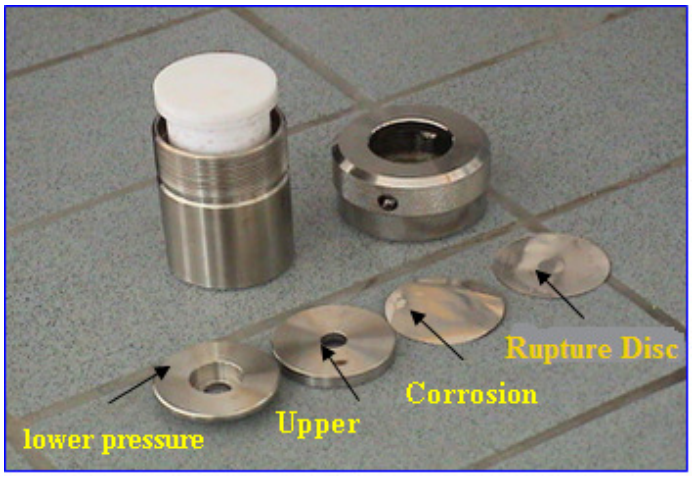

Fig 2.1. Teflon-Lined Stainless Steel Autoclave.

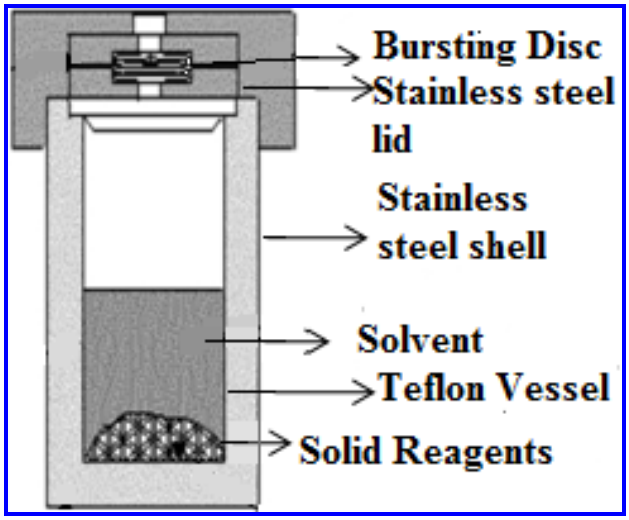

Fig 2.2. Schematic diagram of Teflon-Lined Stainless Steel Autoclave.

The autoclaves are coated with non-reactive Teflon to inhibit corrosion because of its higher coefficient of thermal expansion. Moreover, Teflon will undergo expansion and contraction upon heating and cooling cycles than the loaded materials. Teflon dissociates beyond 300 °C and may affect the pH of the reaction medium. So it cannot be used above 300 °C. The Teflon lining gets torn and thus must be reapplied after some experiments to avoid any discrepancies in the nature of the reaction conditions. Teflon-lined steel autoclave is shown schematically in Figs 2.1 and 2.2.

2.3. Synthesis of the single crystals of metal- organic hybrid complexes

The reaction mixture was pulverized using an agate mortar and pastel (Fig 2.3). The reaction mixture was loaded in a 10 mL Teflon coated stainless steel autoclave and distilled water (4-5 mL) was added, stirred for about 30 min.

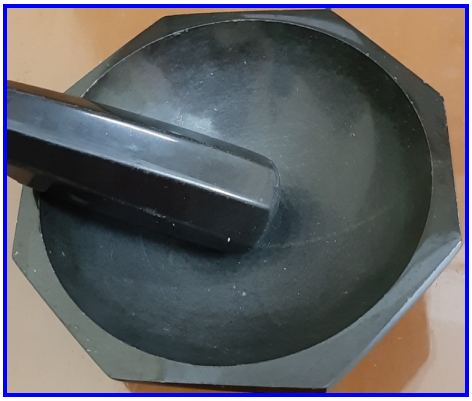

Fig 2.3. Agate mortar and pastel.

Thus a homogeneous suspension was obtained. Then the Teflon vessel was placed inside the bomb body (stainless steel autoclave). The corrosion disc (thinner, next to the Teflon cover) and the rupture disc (thicker, on the outside of sandwich) were placed on top of the liner. After that, the spring with upper and lower pressure plates was added. After adding the spring, the screw cap was attached and turned down firmly by hand. The bomb was placed into an automated hot air oven (Fig 2.4) maintained at a required temperature for a desired time. The autoclave was left for about 6-8 h for natural cooling at room temperature. The pH of the suspension before and after the reaction was recorded.

Fig 2.4. An automated hot air oven.

The reaction mixture was filtered off, washed repeatedly with triply distilled de-ionized water and ethanol; the solid residue was left for air-drying for several hours. Single crystals were then collected by hand picking under a microscope (40x) (Fig 2.5). The single crystals thus obtained were used for single crystal X-ray diffraction study.

Fig 2.5. Compound Microscope.

Mass measurements were carried out on digital electronic analytical balance (Mettler Toledo, AG 285, Switzerland) as shown in Fig 2.6.

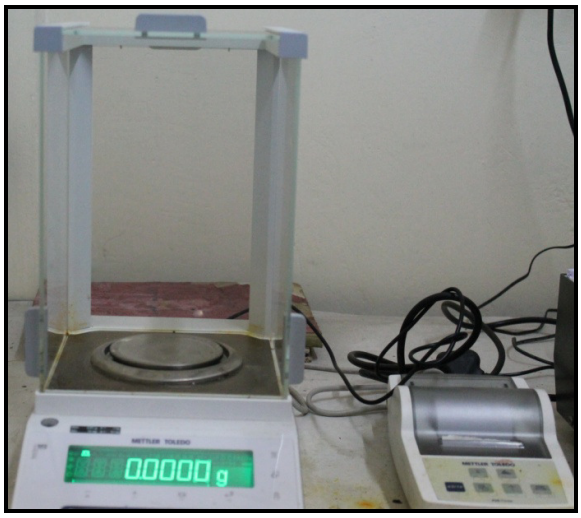

Fig 2.6. Digital electronic analytical balance (Mettler Toledo, AG 285).

This Digital balance can measure mass to a very high precision and accuracy. The mass measurements were accurate to ± 0.01 mg.

2.4. Organic Ligands used

Organic ligands are known for their complex nature and ability to form coordination bonds. They exist mostly in anionic states and, thus, are helpful in forming bonds with metal ions. The common organic ligands used in synthesizing metal-organic hybrid complexes includes benzene-1,3,5-tricarboxylic acid (trivially known as trimesic acid), 1,10-phenanthroline, 3,5-dinitrobenzoic acid, 4-hydroxybezoic acid, picolinic acid, *etc.* The main advantages of organic ligands are their flexibility and tendency to form metal clusters when they coordinates to metal ions. Some organic ligands have the ability to direct crystallization of supramolecular entities through ionic or hydrogen bond interactions between an anionic guest and an organic host. The variety of available carboxylic acids leads to a large number of frameworks with tunable properties. The trianion of trimesic acid plays pivotal role in the field of metal-organic hybrid complexes.

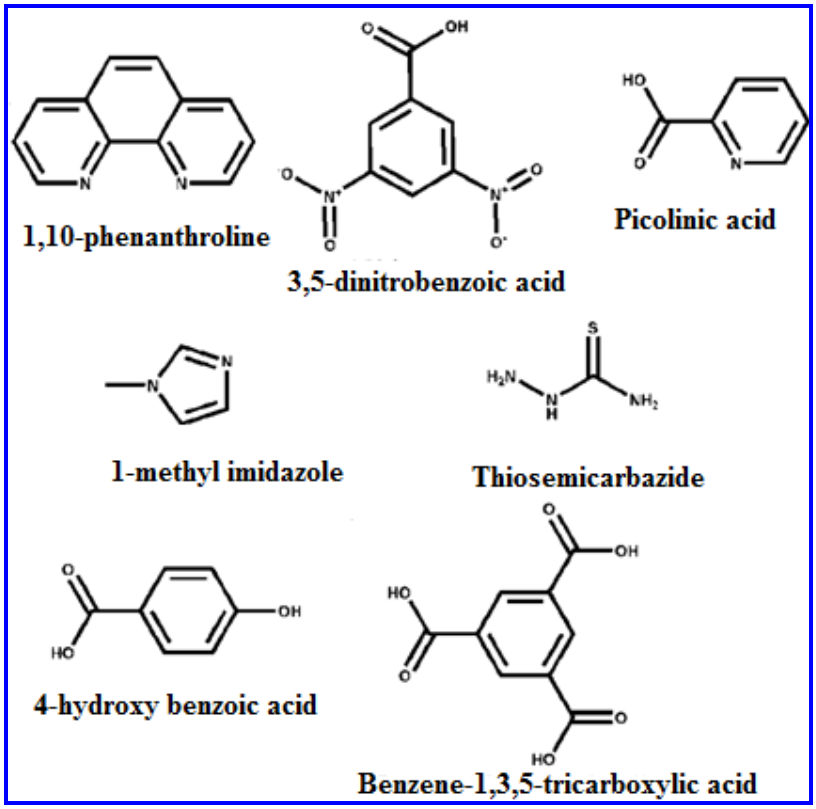

Fig 2.7. Ligands used in the present research work.

2.4.1. 1,10-phenanthroline

Phenanthrolines (phens) are polycyclic aromatic hydrocarbons present in sterols, sex hormones, cardiac glycosides, bile acids, and morphine alkaloids.[1]Among nitrogen heterocycles, phen and their derivatives represent an important class of organic molecules that have attracted considerable interest from both synthetic and medicinal chemists, due to the presence of the phen ring system as a structural pattern in several natural biologically important products, especially alkaloids.

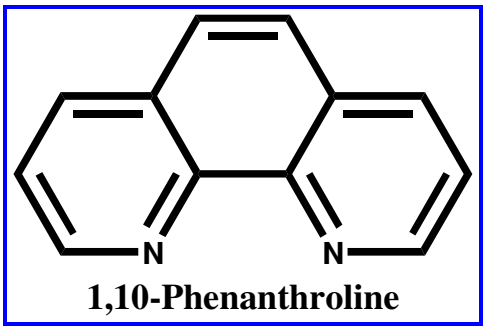

1,10-Phenanthroline

The 1,10-phenanthroline deserves special interest, particularly as a heterocyclic moiety, since in its skeleton the arrangement of the atoms is ideal for chelation of various metal cations, including lanthanide ions. 1,10-phenanthroline have attracted special interest from researchers due to their various structural and chemical properties, *e.g.,* rigidity, planarity, aromaticity, basicity and chelating capability,[2] which makes them versatile starting materials in the area of materials science and in many fields of chemistry; for example, analytical, organic, inorganic, bioorganic, supramolecular coordination, and catalysis chemistry, as well as in the synthesis of photoactive molecules and as a versatile electron transfer reagent.[3-4]

2.4.2. 3,5-dinitrobenzoic acid

3,5-Dinitrobenzoic acid (abbreviated as HDNBA) is the 3,5-dinitro superseded benzoic acid, which has aroused many interests on organic supramolecular architecture and metallorganics for the catalyst, optical and magnetic materials.

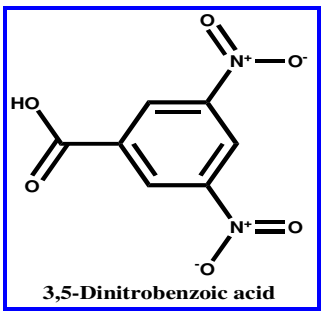

3,5-Dinitrobenzoic acid

In view of the various coordination modes, good thermal stability, high oxygen content, and explosive properties, HDNBA was employed to construct energetic complexes recently.[5-8]

2.4.3. Picolinic acid

Pyridine-2-carboxylic acid (Hpic), has tremendous ability to bind metal atoms like transition metals, alkali metals and even lanthanides. This may be due to its monodentate and bidentate coordinating nature.

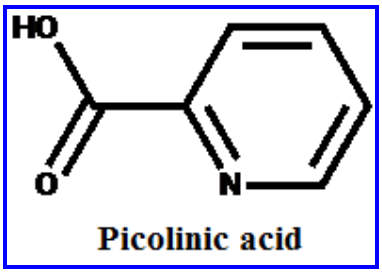

Picolinic acid

In monodentate form it coordinates through either carboxylate O-atom or pyridine N-atom while in bidentate chelating form it uses both the atoms to bind with metal atom and stabilise the complex.[9] The efficient chelation property, allows complexes to show broad spectrum of physiological effects thus can be used in introducing various bioactive metals into the biological system. $Cu(pic)_2$ has been found to be a potential alternative antidiabetic agent[10] and $Cr(pic)_3$ is considered as a popular nutritional supplements.[11] Carboxylate group in picolinate involve in hydrogen bonding and gives supramolecular networks. This plays pivotal role in transmitting magnetic interactions. Recently, polymorphic forms of $Cu(pic)_2$ have been studied intensively for their interesting magnetic properties.[12-14]

2.4.4. 1-methylimidazole

Recently, transition-metal complexes containing imidazole ring have received tremendous attention owing to their riveting applications in catalysis, metal and alloy corrosion inhibition, electrochromic displays, photovoltaic cells and biomaterials.[15-20]

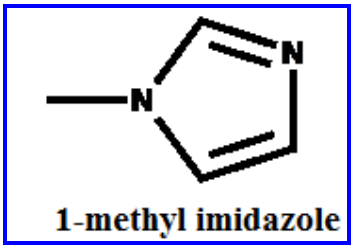

1-methyl imidazole

A remarkable and devoted effort by organic chemists in last 10 years has been observed to design, synthesis, structural characterization and study the diverse applications imidazole-based derivatives.[21-31] The five-membered heterocyclic compounds have been explored for their fascinating physicochemical as well as biological properties. The chemical and thermal robustness, acid-base character, tautomerism, and their facile synthesis and manifold functionalization have attracted chemists across the world. Imidazole is often found as an integral part in large number of medicinally and biologically significant substances.[32-34] In transition metal complexes involving imidazole, the two nitrogen atoms are involved coordination with the metal atom and the chiral auxiliaries at 1, 2, 4 or 5 provides overall asymmetrical environment. These complexes are promising candidates to be used in wide range of asymmetric reactions *e.g.* conjugate addition[35], cyclopropanation,[38] allylation,[37] addition of dialkylzinc to aldehydes,[36] epoxidation and oxidation[39]or transfer hydrogenation.[40]

2.4.5. Thiosemicarbazide

Thiosemicarbazide plays vital role in one's life. Transition metal complexes with hard or soft donor groups have found tremendous in coordination as well as Organometallic Chemistry.[41] In most of the complexes thiosemicarbazones, condensation derivative of thiosemicarbazide and aldehydes or ketones behave as bidentate ligands. They coordinate metals through hydrazinic nitrogen atoms and sulphur atom. Although in some cases they act as unidentate ligands and coordinates through sulphur atom only.[42-43]

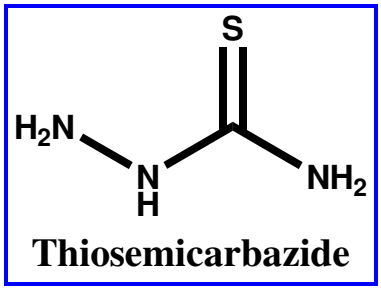

Thiosemicarbazide

The thiosemicarbazone molecules form chelate with even trace amount of metals in the biological system and thus give it an identity to be effective carrier of bioactive molecules. Metal complexes involving thiosemicarbazones have been explored for about 50 years [44-45] because of their versatile biological activity and prospective use as drugs.[46] This huge interest over the years is due to the potential biological properties

and used as prospective drugs like antitumour,[48] anticancer,[47] antimalarial,[51] antiviral[52] antifiungal[49] antibacterial[50] and anti-HIV.[53] The hypoxic selectivity of copper bis(thiosemicarbazones) which is used as modes for delivering radioactive isotopes of copper to tumors[54] or leucocytes[55] has gained recent attention.

2.4.6. 4-hydroxybenzoic acid

Metal arylcarboxylates being biologically important compounds have shown verstile coordination modes[56-63] such as ionic, monodentate, bidentate bridging(both symmetric or unsymmetric) as well as bidentate chelating.[64-65]

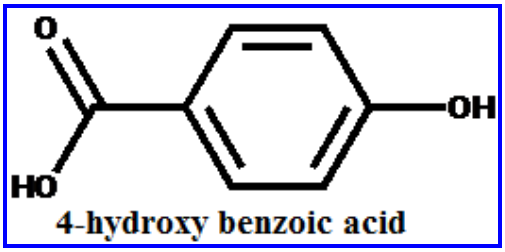

4-hydroxy benzoic acid

The hydroxy-, nitro- and amino-derivatives of benzoic acid are found to be useful in the fields cosmetics, engineering, food industry, *etc.*[66-68]

2.4.7. Benzene-1,3,5-tricarboxylic acid (Trimesic acid, TMA)

Benzene-1,3,5-tricarboxylic acid is rigid, planar molecule has been utilized extensively due to their rigidity and versatile coordination modes towards the metal ions.

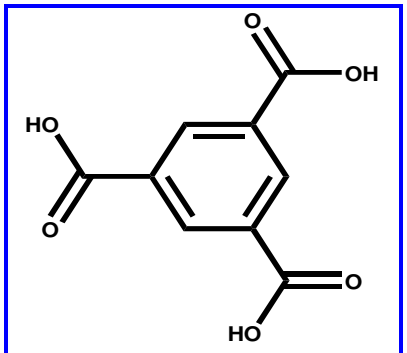

Benzene-1,3,5- tricarboxylic acid

Among polycarboxylates, 1,2,4,5-benzenetetracarboxylic, 1,3,5-benzenetricarboxylic, 1,2,3 benzenetricarboxylic, and 1,4-benzenedicarboxylic have been used frequently resulting in fascinating molecular geometries and connectivity.[69-72] with diverse frameworks ranging from 1D to 3D.[73-74]

2.5. Solvents and Temperature

The syntheses of the metal-organic hybrid complexes are performed by hydrothermal method that uses water as solvents for the purpose of dissolving reactants. Pure solvents or mixture of solvents can also be used. The solutions containing the reactants are kept in Teflon cups in an autoclave for faster processing. The autoclave is allowed to run for few hours to several days to allow crystal growth depending on the rate of reaction. Usually high temperatures (160- 240 °C) are used for running the reactions in autoclaves. Low temperatures ranging from 25-120 °C can be used for reactions containing pure organic solvents that are volatile. The frameworks contain coordinated solvent molecules in their pores that can be removed to give porous materials and the empty spaces within the MOF form unsaturated open metal sites. These unsaturated open metal sites and large pores are helpful in various applications such as gas adsorption and gas separation.

2.6. Physico-chemical characterization

The physico-chemical characterization of the synthesized hybrid complexes was performed by various physico-chemical methods as discussed below:

2.6.1. Elemental analysis

The micro-elemental analysis (CHN) of the synthesized complexes was performed on a Perkin–Elmer (Model 240C) analyzer.

Fig 2.8. Atomic Absorption Spectrophotometer (Varian SpectrAA 50B).

The metal content in the complexes were determined using Atomic Absorption Spectrophotometer (Varian SpectrAA 50B). It was calibrated with Sigma-Aldrich standards for a particular metal and concentration determinations were done with weighted amount of the complexes digested in concentrated nitric acid and diluted to definite volumes. Fig 2.8. shows the AAS instrument used for the analysis of metal contents in the complexes**.**

2.6.2. Infrared spectroscopy (FTIR)

FT–IR spectra of the synthesized hybrid complexes were recorded as either KBr pellets with Perkin-Elmer FT-IR spectrophotometer (RX-1) in the range 400-4000 cm^{-1}. Fig 2.9 shows the Perkin–Elmer FT-IR spectrophotometer (RX-1) used.

Fig 2.9. Perkin–Elmer FT-IR spectrophotometer (Spectrum RX-1).

A pinch of the sample was first pulverized with KBr in approximately a 1:10 ratio and placed in to press hydraulically and a pellet was obtained. The pellet was then loaded inside the port of the spectrometer. The measurements were then carried out at an optimized resolution of 8 cm^{-1}. A total of 20 scans were done. The obtained spectrum was subjected to baseline correction and then it was interpreted analytically for the synthesized complexes.

2.6.3. Nuclear Magnetic Resonance (NMR) spectroscopy

^{1}H-NMR spectra of the synthesized derivatives of benzimidazole discussed in chapter VI were recorded at room temperature using FT-NMR (Bruker Avance-II 400 MHz) spectrometer by using DMSO-d_6 as solvents. The chemical shifts (recorded in ppm) downfield of internal standard tetramethylsilane (TMS). The nuclear magnetic resonance spectrometer Avance II 400 is a high-field NMR spectrometer with a 9.4 Tesla superconducting magnet operating at a nominal ^{1}H frequency of 400 MHz.

2.6.4. Mass spectroscopy

The mass spectra of the synthesized compounds have been analyzed using WATERS Q-TOF Premier HAB-213 mass spectrophotometer in methanol solvent.

2.6.5. Electron paramagnetic resonance (EPR) spectroscopy

The X-band EPR data of the synthesized single crystals of the complex was studied using EPR magnetometer (JEOL, JES-X3 FA200) in the field range of 266.66 to 386.66 mT. JEOL JES FA200 instrument, as shown in Fig 2.10, is Electron Spin Resonance (ESR) spectrometer used for the species containing unpaired electrons (transition metal complexes, free radicals, rare earth ions, odd-electron molecules, *etc.*)

Fig 2.10. JEOL, JES-X3 FA200 EPR spectrometer.

The continuous wave (CW) ESR spectrometer is based on field modulation and phase sensitive detection. The Microwave Bridge contains the Gundiode, acting as source of the radiation and the Detector. The specimen/sample to be analyzed was placed in a resonant cavity that admits microwaves through iris. The resonant cavity located in the centre of electromagnet amplifies the weak signals coming from the sample. The

performance of the instrument is enhanced by other components such as field modulator, attenuator, and amplifier included in the instrument. The nature of hyperfine interactions of low magnitude can be studied using X-Band ENDOR facility available with this instrument. This may also be used for complete understanding of the electronic structure of the molecule. The block diagram of JEOL, JES-X3 FA200 EPR spectrometer is shown in Fig 2.11.

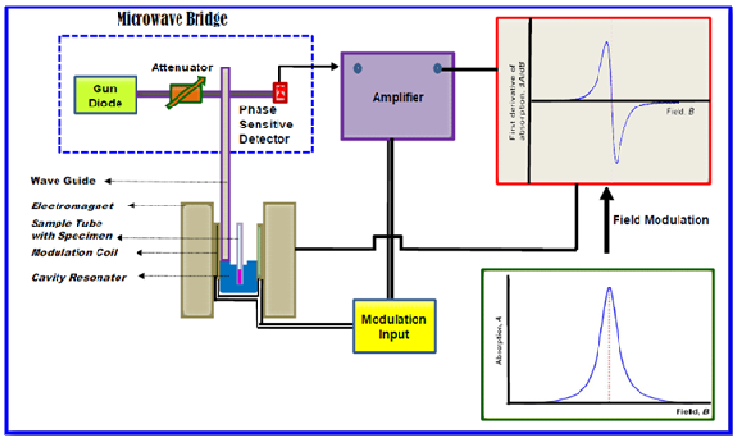

Fig 2.11. Block diagram of JEOL, JES-X3 FA200 EPR spectrometer

The measurement of the *g*-factor (centre of the spectrum) and the hyperfine splitting (interaction between nuclei with spin $I \neq 0$) can also be monitored using this instrument. Fine structure/Zero-field splitting characteristic of transition metal complexes and other species containing two or more unpaired electrons ($S \geq 1$) can also be observed from solid samples.

2.6.6. X-ray Diffraction

2.6.6.1. Single Crystal X-ray Diffraction

Single crystal X-ray diffraction methods have several applications such as determination of unit cell, space group, crystal structure, electron distribution, atom size and bonding, crystal defects and disorder. The immense role played by X-ray diffraction in the determination of crystal structure of various solids cannot be exaggerated. Virtually all the knowledge about crystal structures has been obtained by X-ray diffraction for about sixty years. This essential knowledge has helped to understand crystalline materials, their structures, properties and applications. High-precision structural results require dislocation free single crystals. In general, crystals should meet the following criteria:

i) The crystals must be single entity with neither powder nor smaller crystals attached to it.

ii) They should be of the proper shape and size with well-defined lustrous faces and should have uniform color with no cracks.

iii) The crystals should diffract reasonably with high scattering angles.

Diffraction patterns can be obtained from a single crystal instead of the randomly oriented crystals that are found in a powder. From a single crystal the position and intensity of the *hkl* reflections can be measured accurately and from this data the space group and the precise atomic positions of the crystal can be determined. The information that can be obtained includes: crystal symmetry, unit cell dimensions, details of site ordering, atomic positions and space group. These unit cell parameters have been used to verify if a structure is new or known in the literature. A single crystal was mounted vertically on a goniometer so that it can be rotated about one of the crystallographic axes. The diffraction from each plane lies on the surface of a set of cones. Each plane is brought into the diffraction condition by rotating the crystal. The reflections can be recorded on a film wrapped around the rotating crystal. Finally the intensity of all the reflections was measured. This measurement provides all the data necessary to solve the crystal structure.

Single crystal X-ray diffraction data were collected on an Oxford diffractometer (with Mo Kα, wavelength = 0.71069 Å) equipped with CCD camera and an Oxford Cryosystem open-flow nitrogen cryostat with a normal stability of 0.1 K. An absorption multiscan[75] or analytical correction[76] was applied to all the data and analyzed with related softwares.[77] The structure of the synthesized complex was solved by direct methods using SIR97 programme[78] in combination with Fourier difference synthesis. The structure was refined against F or F2 using CRYSTAL program.[79] All the H-atoms were located in a difference Fourier map but those attached to C-atoms were repositioned geometrically. The H-atoms were initially refined with soft constraints on the bond lengths (C-H = 0.93-0.98, N-H 0.86-0.89 and O-H = 0.82 Å) and angles to regularize their geometry with U_{iso} (H) in the range 1.2-1.5 times U_{eq} of the parent atom, after which the positions were refined with a riding constraints.[80] All non-hydrogen atoms were refined with anisotropic displacement parameters.

Single crystal X-ray diffraction of compound discussed in chapter VI was carried out on an Oxford Diffraction Xcalibur 3/Sapphire3 CCD diffractometer (manufactured by Oxford diffraction, Poland) equipped with CCD (with Mo Kα, λ=0.71073 Å) at 299 K using ω scan technique. Data refinement and reduction were carried out using CrysAlis*PRO*(Agilent Technologies, version 1,171.37.35, 2014). The crystal system was determined by Laue symmetry and the space groups was assigned on the basis of systematic absences using XPREP.The structure was solved by direct method using the SHELXS program of the SHELXTL package and refinedon F^2 by full-matrix least-squares methods with SHELXL-2014.crystallographic software package.[81] All the non-hydrogen atoms were anisotropically refined and all hydrogen atoms were placed in the calculated positions and refined isotropically with a rigid model. The hydrogen atoms bound to water molecules were found via Fourier difference map and these hydrogen atoms were then restrained at fixed positions and refined isotropically. The crystal of copper (II) complex was twinned (inversion); its twin law was found via TWIN/BASF instructions included in the SHELXL2014 instruction file (Sheldrick, 2015).[82] All calculations and molecular graphics were carried out with the SHELXL-2014/7 PC programme package and ORTEX.[83]

2.6.6.2 Powder X-ray Diffraction

This instrument comes with unique CRISP technology, pneumatic shutters and beam attenuators. The X′Pert Powder Diffractometer is very much reliable and guarantees smooth operation over the systems lifetime and low running cost.

Fig 2.12. Pan analytical X′pert powder X-ray Diffraction (PXRD).

The 2nd generation versatile PreFIX technology is easy to use. The X′Pert Powder can be equipped with cost-effective detector (sealed Xe proportional detector) and scintillation detector is suited for hard radiation applications such as pair distribution function analysis. The X′Celerator comes with 128 channels of 70 µm gives you superior resolution. Without the need for cooling water, liquid nitrogen flow, counting gas or calibrations it is a very cost-effective solution.

2.6.7. Thermo Gravimetric Analysis

Thermo Gravimetric Analysis (TGA) is used to study the thermal stability of the complex that involves both which physical and chemical changes taking place within a compound with rise in temperature as well as change of mass of the compound. It includes both material transition and thermal degradation and helps in the determination of decomposition and thermal stability of products of a material. Thermo Gravimetric Analysis (TGA) measures changes in the mass/weight of samples as a function of temperature. TGA is commonly used for the determination of degradation temperatures, absorbed moisture, residual solvent level, and also the amount of non-combustible inorganic fillers present in the composite materials. The sample is placed in a tarred TGA sample pan, attached to sensitive microbalance assembly. The sample holder of the TGA balance assembly is placed into a high temperature furnace. The balance assembly first measures the initial weight of the sample at room temperature and then monitors continuously the changes in sample weight with increasing supply of heat to the sample. The thermal stability of the complex was studied by thermogravimetric (TGA) and Differential Thermogravimetry (DTG) analysis. The thermal data of the reported complexes were recorded using TGA instrument (Q500 V20.10 Build 36) in N_2 atmosphere with an initial weight of the complex subjected to a heating rate of 10 °C·min^{-1}.

2.6.8. Magnetic susceptibility measurement

The magnetic susceptibility measurements were done at room temperature on a Sherwood Scientific Ltd magnetic susceptibility balance (Magway MSB Mk1). The working principle of MSB is based on moving magnets and stationary sample. The pair of magnets present at opposite ends of a beam to keeps the system balanced. The sample when introduced between the poles of a pair of magnets produces deflection of the beam that is registered by phototransistors. A current is allowed to pass through the coil mounted between the poles of another pair of magnets produces force

restoring balance of the system. At equilibrium, the current passing through the coil is proportional to the force exerted by the sample that is measured as voltage drop. Fig 2.13 shows the magnetic susceptibility balance used.

Fig 2.13. The Magnetic Susceptibility Balance (MSB).

The sample is first tightly packed in a weighed sample tube of suitable length (*l*) and the sample weight (*m*) was noted. Then this packed tube was placed in a tube guide of the balance and the reading (*R*) was noted. The mass susceptibility, χ_g, was calculated using:

$$\chi_g = C_{Bal} \times l \times \frac{(R - R_0)}{m \times 10^9} \qquad (1)$$

where l = length of the sample (in cm), m = mass of the sample (in g), R_0 = reading of the empty tube, R = reading of the tube with sample, and C_{Bal} = balance calibration constant. Thus the molar susceptibility of the reported compounds can be calculated using the formula $\chi_M = \chi_g \times$ Molecular weight of the sample. The molar susceptibility was corrected with diamagnetic contributions. The effective magnetic moment, μ_{eff} was calculated by using the following expression:

$$\mu_{eff} = 2.83\sqrt{T \times \chi_A} \quad \text{B.M.} \qquad (2)$$

where χ_A is the corrected molar magnetic susceptibility. The MSB was calibrated with Hg $[Co(SCN)_4]$.

2.6.9. SQUID Magnetometry

SQUID magnetometer is the only method used directly for the determination of overall magnetic moment of samples in absolute units.

Fig 2.14. Ever Cool 7 Tesla SQUID magnetometer.

Magnetic susceptibility data of the reported complexes were collected on powdered crystalline sample using SQUID magnetometer (Ever Cool 7 Tesla). For the measurements, the crystalline sample was first pulverized and then packed in a pre-calibrated quartz tube. The susceptibility data were obtained at 100 *Oe* in the temperature range of 2 to 300 *K*. The susceptibility data were corrected for the sample holder previously measured under the same conditions and also the diamagnetic contributions of the sample using Pascal's constants.[84]

2.6.10. Field Emission Scanning Electron Microscopy (FESEM) The crystal morphology was studied using Field Emission Scanning Electron Microscopy [FESEM, INSPECT F50 (FEI, The Netherland)].

Fig 2.15. FESEM, INSPECT F50 (FEI, The Netherland).

The basic principle of SEM is that beam of electrons are generated by a tungsten filament or field emission gun.

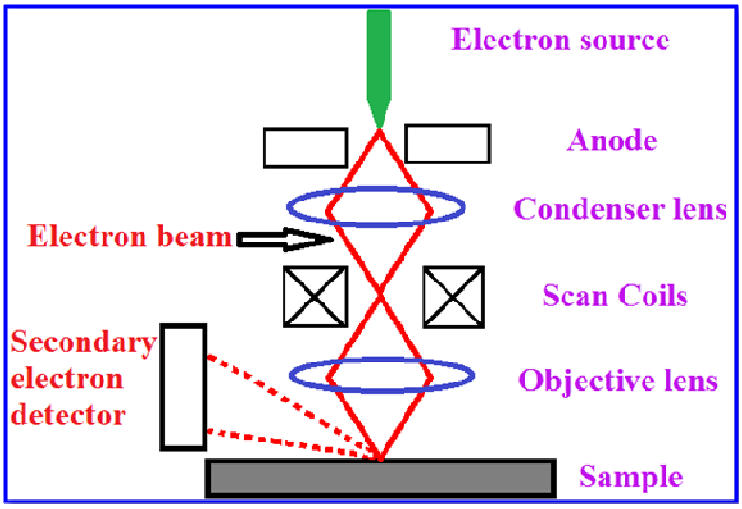

Fig 2.16. Block diagram of FESEM.

The electron beam gets accelerated through a high voltage (*e.g.,* 20 kV) and then passes through the system of electromagnetic lenses and apertures and produces a thin beam of electrons. The beam then scans the surface of the specimen by scan coils. The scanning beam allows the emission of electrons from the surface of specimen that is collected by a detector. The series of lenses in a vacuum chamber of the microscope directs the electrons towards the specimen in order to maximize efficiency. The more the electrons used, the more powerful will be the magnification.

When a specimen is hit with a beam of electrons known as incident beam, it emits X-rays and three kinds of electrons: primary backscattered, secondary and Auger electrons. The SEM uses only primary backscatter and secondary electrons.

2.7. Theoretical characterization

The theoretical characterizations of the complexes were performed using Gaussian 09 programme package. The molecular structures of the synthesized complexes were optimized by the DFT method using B3LYP hybrid functional[85-86] combined with LANL2DZ basis sets for ligands and metal ion respectively. One of the prominent features of the LANL2DZ basis set is its inclusion of relativistic effect that is prerequisite for heavy elements. The total energy calculations within the DFT framework were carried out to ascertain the interaction of metal ion with the ligand coordination environment. The optimized structures, vibrational frequencies, electronic spectra, HOMO-LUMO energies, chemical potential (μ), Global hardness (η) and global electrophilicity power (ω), Mulliken charge and MESP properties are the main theoretical assessments carried out for the complexes. The Hirschfield surface analysis has been carried out to explore the types of intermolecular interactions prevailing in the molecule using crystal explorer 17.5 programme.[87]

2.7.1. DFT study

The geometrical structure of the complex was optimized at B3LYP level of theory using LANL2DZ basis set and it has been found that the optimized geometry of the complex is consistent with the structure obtained from single crystal X-ray diffraction study.

2.7.2. Frontier molecular orbitals

The Frontier Molecular Orbitals (HOMO and LUMO) can qualitatively predict the excitation properties and electron transport in the studied system and in this context the parameters HOMO and LUMO offers reasonable prediction of the molecular reactivity. Thus the energies of the HOMO and LUMO of the complex have been calculated using density functional theory (DFT). The DFT based descriptors (HOMO-LUMO orbital energy) could be used in order to understand the structure and reactivity of molecule by calculating different properties such as Chemical potential (μ), Global hardness (η) and global electrophilicity power (ω). The HOMO-LUMO orbital energies are directly related to ionization energy ($I= -E_{HOMO}$) and electron affinity ($A= -E_{LUMO}$). Similarly, the chemical potential (μ), Global

hardness (η) and global electrophilicity power (ω) are related to HOMO-LUMO orbital energies by the following relations: chemical potential (μ)= (E_{HOMO}+E_{LUMO})/2, Global hardness (η) = (-E_{HOMO}+E_{LUMO})/2 and global electrophilicity power (ω) = $\mu^2/2\eta$. Alternatively, chemical potential (μ) and Global hardness (η) are given by the following relations: μ= -(I+A)/2 and η=(I-A)/2. Where I and A are the first ionization potential and electron affinity of the chemical species.

2.7.3. Mulliken charges

Atomic charge of a molecular system is an important parameter; thus the calculation of atomic charges has an important role in quantum mechanical calculations. The mulliken charges are a function of electron density population and thus, the mulliken charges are usually calculated by determining the electron population of each atom as defined in the basis function.

2.7.4. Molecular Electrostatic Potential

The Molecular Electrostatic Potential surface diagram was used to study the reaction behavior of a molecule. The negative regions of the MESP are regarded as nucleophilic centers, while the positive regions as potential electrophilic sites. MESP an Electron Density dependent property and is a valuable descriptor for understanding electrophilic and nucleophilic sites and also hydrogen bond interactions. Hence an electrophilic and nucleophilic reactive site for the reported complex was studied at the B3LYP/LANL2DZ optimized geometry was calculated.

2.7.5. Hirschfeld surface analysis: In order to quantify the various intermolecular interactions, Hirschfeld surface analysis[88] has been carried out for the synthesized complex and their associated two-dimensional fingerprint plots have been used to predict the possible intermolecular interactions. The descriptor d_{norm}, which incorporates two factors: (i) d_e, signifying the distance of any surface point nearest to the internal atoms, and (ii) d_i, signifying the distance of the surface point nearest to the exterior atoms and also with the van der Waals radii of the atoms has been used for mapping the Hirschfeld surface of a molecule.[89] The parameter d_{norm} is given by a mathematical expression as: $d_{norm} = (d_i - r_i^{vdw})/r_i^{vdw} + (d_e - r_e^{vdw})/r_e^{vdw}$, where r_i^{vdw} and r_e^{vdw} are the van der walls radii of the atoms. The parameter d_{norm} may have negative or positive value depending on the types of intermolecular contacts.[90] If the

value is positive, then the intermolecular contacts are shorter and if the value is positive the contacts are larger than the van der walls separations.[91] The descriptor d_{norm} displays a surface with bright red, white and blue spots for shortest contact, contact around the van der walls separation and devoid of close contacts respectively. Crystals with spherical atomic electron densities, the Hirschfeld surface is unique and it gives an idea about the intermolecular interactions occurring in the studied molecular crystals.[92] In order for better visualization of the molecular moiety around which they are calculated, the surfaces have been shown as transparent.[93]

2.8. Catalysis

Among the various nitrogen based heterocyclic compounds, benzimidazole scaffold because of their wide range of biological activities are ubiquitous in nature and these are often useful bioactive intermediates for the preparation of pharmalogical and biological active molecules. In literature, variety of methods for the synthesis of 2-substituted benzimidazoles using ortho-phenylenediamines and aldehydes as precursors has been reported. Those methods require long reaction time, expensive organic solvents and catalysts. The synthesis of 2-arylbenzimidazoles in solvent free condition using silica gel as a solid medium is an efficient, eco-friendly and greener approach. So to develop a solvent free green reaction condition for synthesizing 2-substituted benzimidazole using ortho-phenylenediamine and aromatic aldehyde as precursors over silica gel (TLC grade) in open air was carried out. In order to optimize the catalyst and reaction conditions, 1,2-phenylenediamine (1mmol) and 2-nitrobenzaldehyde (1mmol) were taken as precursors for initial model reaction. The feasibility of the developed methodology was scrutinized for a series of aryl and heteroaryl aldehydes and it has been found that all the aldehyde gave excellent yield up to 98% under the reaction condition. The spectral data of the synthesized benzimidazole derivatives are in full agreement with data reported in the literature. The yield and spectral data of compounds are summarized in tabular form. The recyclability of the catalyst was then investigated and it has been found that the catalyst can be recovered after completion of the reaction and it can be used further up to 5th run with no significant loss of activity.

References

[1]. L. Castedo and G. Tojo, *The Alkaloids: Chemistry and Pharmacology,* Brossi, *A., Ed., Academic Press,* 1990, **39**, 99.

[2]. I. J. Villar-Garcia, A. Abebe, *Inorg. Chem.Commun.* 2012, **19**, 1.

[3]. G. Accorsi, A. Listorti, K.Yoosaf, *Chem. Soc. Rev.,* 2009, **38,** 1690.

[4]. A. Bencini and V. Lippolis, *Coord. Chem. Rev.* 2010, **254**, 2096.

[5]. M. Kaur, H. S. Yathirajan, K. Byrappa, E. Hosten and R. Betz, *Z. Kristallogr. NCS,* 2014, **229**, 488.

[6]. X. Liu, Q. Yang, Z. Su, S. Chen, G. Xie, Q. Wei and S. Gao, *RSC Adv.,* 2014, **4,** 16087.

[7]. X. Liu, Z. Su, W. Ji, S. Chen, Q. Wei, G. Xie, X. Yang and S. Gao, *J. Phys. Chem. C.,* 2014, **118,** 23487.

[8]. F.A. Mautner and S.S. Massoud, *J. Mol. Struct.,* 2007, **871,** 108.

[9]. D.R. Finch, P.J. Morris and R.I. Vanhegan, *Transplantation*, 1977, **23**, 182.

[10]. S. Chaudhary, J. Pinkston, M.M. Rabile and J.D. Van Horn, *J. Inorg. Biochem.,* 2005, **99,** 787.

[11]. M.S. Kanth and A. Mishra, *Orient. J. Chem.*, 2005, **21**, 537.

[12]. B. Zurowska, J. Ochocki, Z. Ciunik, J. Mrozin´ ski and J. Reedijk, *Inorg. Chim. Acta*, 2004, **357**, 755.

[13]. B. Z_urowska, J. Mrozin´ ski and Z. Ciunik, *Polyhedron*, 2007, 26, 1251.

[14]. R. J. Sundberg and B. Martinb, *Chem. Rev*., 1974, **74**, 471.

[15]. R.N. Patel and K.B. Pandeya, *J. Inorg. Biochem.*, 1998, **72**, 109.

[16]. R.J. Hodgkiss, G.W. Jones, A. Long, R.W. Middleton, J. Parrick, M.R.L. Stratford, P.Wardman and G.D. Wilson, *J. Med. Chem*., 1991, **34**, 2268.

[17]. J. Brown, I. Hamerton and B.J. Howlin, *J. Appl. Polym. Sci.*, 2000, **75**, 201.

[18]. H. Ohtsu, Y. Shimazaki, A. Odani, O. Yamauchi, W. Mori, S. Itoh and S. Fukuzumi, *J. Am.Chem. Soc*., 2000, **122**, 5733.

[19]. F. Ragot, S. Belin, V. Ivanov, D.L. Perry, M. Ortega, T.V. Ignatova, I.G. Kolovov, E.A. Masalitin, G.V. Kamarchuk, A.V. Yeremenko, P. Molinie, J. Wery and E. Faulques, *Mater. Sci*., 2002, **20**, 13.

[20]. F. Corelli, V. Summa, A. Brogi, E. Monteagudo and M. Botta, *J. Org. Chem.,* 1995, **60**, 2008.

[21]. M. Groarke, M. A. McKervey and M. Nieuwenhuyzen, *Tetrahedron Lett.* 2000, **41**, 1275.

[22]. T. Rűther, M. C. Done, K. J. Cavell, E. J. Peacock, B. W. Skelton and A. H. White, *Organometallics,* 2001, **20**, 5522.

[23]. F. Bureš and J. Kulhánek, *Tetrahedron Asymmetry,* 2005, **16,** 1347-1354.

[24]. H. Y. Jiang, C. H. Zhou, K. Luo, H. Chen, J. B. Lan and R. G. Xie, *J. Mol. Catal. A: Chem.,* 2006, **260,** 288-294.

[25]. Y. Matsuoka, Y. Ishida, D. Sasaki and K. Saigo, *Tetrahedron,* 2006, **62**, 8199-8206.

[26]. A. Marek, J. Kulhánek, M. Ludwig and F. Bureš, *Molecules,* 2007, **12,** 1183-1190.

[27]. P. J. Thomas, A. T. Axtell, J. Klosin, W. Peng, C. L. Rand, T. P. Clark, C. R. Landis and K. A. Abboud, *Org. Lett.,* 2007, **9,** 2665-2668.

[28]. A. V. Gulevich, E. S. Balenkova and V. G. Nenajdenko, *J. Org. Chem.,* 2007, **72,** 7878.

[29]. G. Mlostoń, P. Mucha, K. Urbaniak, K. Broda and H. Heimgartner, *Helv. Chim. Acta,* 2008, **91**, 232.

[30]. B. S. Gerstenberg, J. Lin, Y. S. Mimieux, L. E. Brown, A. G. Oliver and J. P. Konopelski, *Org. Lett.,* 2008, **10**, 369.

[31]. De Luca and L. Curr, *Med. Chem.,* 2006, **13**, 1.

[32]. M. Boiani and M. González, *Mini-Rev. Med. Chem.,* 2005, **5**, 409-4.

[33]. J. Suwiński, W. Szczepankeiwicz, K. Świerczek and K. Walczak, *Eur. J. Org. Chem.,* 2003, 1080-1084.

[34]. I. Katsuki, Y. Motoda, Y. Sunatsuki, N. Matsumoto, T. Nakashima and M. Kojima, *J. Am. Chem. Soc.,* 2002, **124**, 629.

[35]. L. Hojabri, A. Hartikka, F. M. Moghaddam and P. I. Arvidsson, *Adv. Synth. Catal.,* 2007, **349,** 740.

[36]. H. Kotsuki, H. Hayakawa, M. Wakao, T. Shimanouchi and M. Ochi, *Tetrahedron Asymmetry,* 1995, **6,** 2665.

[37]. N. R. Perl and J. L. Leighton, *Org. Lett.,* 2007, **9,** 3699.

[38]. H. Shitama and T. Katsuki, *Chem. Eur. J.,* 2007, **13,** 4849.

[39]. M. Gullotti, L. Santagostini, R. Pagliarin, A. Granata and L. Casella, *J. Mol. Catal. A: Chem.,* 2005, **235,** 271.

[40]. R. Hodgson and R. E. Douthwaite, *J. Organomet. Chem.* **2005**, *690*, 5822.

[41]. A. R. Sarkar and S. Mandal, *Synth React Inorg Met-Org Chem.*, 2000, **80**, 1477.

[42]. S. Padhye and G.B. Kauman, *Coord. Chem. Rev*., 1985, **63**, 127.

[43]. A. R. Cowley, J. R. Dilworth, P.S. Donnelly, E. Labisbal and A. Sousa, *J. Am. Chem. Soc.,* 2002, **124**, 5270.

[44]. G.V. Bahr and G. Schleizer, *Z. Anorg. Chem.* 1955, **280**, 161.

[45]. D.L. Klayman, J.P. Scovill, J.F. Bartosevich and J.Bruce, *J. Med. Chem.,* 1983, **26,** 35.

[46]. V. Philip, V. Suni, M.R.P. Kurup and M. Nethaji, *Polyhedron*, 2006, **25**, 1931.

[47]. F.A. French and E.J. Blanz Jr., *J. Med. Chem.* 1996, 9, 585.

[48]. M. Das and S.E. Livingstone, *Br. J. Cancer*, 1978, **37**, 466.

[49]. A. S. Dobek, D. L. Klayman, L. T. Dickson, J. P. Scovill and E. C. Tramont, *Antimicrob. Agents Chemother.,* 1980, **18**, 27.

[50]. A. Usman, I. A. Razak, S. Chantrapromma, H. K. Fun, A. Sreekanth, S. Sivakumar and M. R. P. Kurup, *Acta Cryst. C*, 2002, 461.

[51]. D. L. Klayman, A. J. Lin and J. W. McCall, *J. Med. Chem.*, 1991, **34**, 1422.

[52]. A. K. El-Sawaf, D. X. West, R. M. El-Bahnasawy and F.A. E1-Saied, *Transition Met. Chem.,* 1998, **23**, 227.

[53]. N. Takahashi, Y. Fujibayashi, Y. Yonekura, M. J. Welch, A. Waki, T. Tsuchida, N. Sadato, K. Sugimoto and H. Itoh, *Ann. Nucl. Med.,* 2000*,* **14**, 323.

[54]. M. D. Yu, M. A. Green, B. H. Mock and S. M. Shaw, *J. Nucl. Med.,* 1989, **30** 920.

[55]. C. J. Anderson and M. J. Welch, *J. Chem. Rev.,* 1999, **99**, 2219.

[56]. A. Mautner, R. Vicente, F. R.Y. Louka and S. S. Massoud, *Inorg. Chim. Acta*, 2008, **361**, 1339.

[57]. V. Zelenak, M. Sabo, W. Massa and P. Llewellyn, *Inorg. Chim. Acta*, 2004, **357,** 2049.

[58]. P. Stachova, M. Melník, M. Korabik, J. Mrozinski, M. Koman, T. Glowiak and D. Valigura, *Inorg. Chim. Acta*, 2007, **360**, 1517.

[59]. M. Iqbal, S. Ali, Z.-U. Rehman, N. Muhammad, M. Sohail and V. Pandarinathan, *J. Coord. Chem*., 2014, **67**, 1731.

[60]. A. Erdelyiova, K. Gyoryova, R. Gyepes, L. Halas and J. Kovarova, *Polyhedron,* 2009, **28**, 131.

[61]. J. Zhao, *Acta Crystallogr*, 2008, **64**, 1321.

[62]. F.E. Ozbek, B. Tercan, E. Sahin, H. Necefoglu, T. Hokelek, *Acta Crystalogr.,* 2009, **65**, 341.

[63]. Y. J. Cai, X. Zhou, Z. Gui, and Y.G. Li, *New Cryst. St.,* 2010, **225**, 361.

[64]. R.P. Sharma, A. Singh, A. Saini, P. Venugopalan, A. Molinari and V. Ferretti, *J. Mol. Struct.,* 2009, **923**, 78.

[65]. K. Eschrich, F. J. T. van der Bolt, A. de Kok, W. J. H. van Berkel, *Eur. J. Biochem.,* 1993, **216**, 137.

[66]. A. Q. Ashton, *Benzoic Acids—Advances in Research and Application*, Ed. *by (Scholarly Editions, Atlanta, USA,* 2013*).*

[67]. M. Frauenkron, J. P. Melder, G. Ruider, *Ullman's Encyclopedia of Industrial Chemistry*, 2012, **13**, 405.

[68]. H. Z. Zardini, M. Davarpanah and M. Shanbedi, *Biomed. Mater. Res. A*, 2014, **102**, 1774.

[69]. S. M. Roy, M. R. Sudarsanakumar and V. S. Dhanya, *J. Korean Chem. Soc.,* 2014, **58**, 258.

[70]. M. Li, L. Liu, L. Zhang, X.F. Lv, J. Ding, H.W. Hou and Y.T. Fan, *CrystEngComm*., 2014, **16**, 6408.

[71]. G. Wu, J. H. Feng and X. F. Wang, *Z. Anorg. Allg. Chem.,* 2012, **638**, 1047.

[72]. X. P. Zhang, J. M. Zhou, W. Shi, Z. J. Zhang and P. Cheng, *CrystEngComm.*, 2013, **15,** 9738.

[73]. L.F. Ma, B. Liu, L.Y. Wang, J.L. Hu, M. Du, *Cryst.Eng.Comm.,* 2010, **12**, 1439.

[74]. O. M. Yaghi, G. M. Li and H. L. Li, *Nature,* 1995, **378**, 703.

[75]. O. M. Yaghi, H. L. Li and T. L. Groy, *J. Am. Chem. Soc.,* 1996, **118,** 9096.

[76]. O. M. Yaghi, C. E. Davis, G. M. Li and H. L. Li, *J. Am. Chem. Soc.,* 1997, **119**, 2861.

[77]. CRYSALISPRO, Oxford Diffraction Ltd., Version 1.171.33.46 (release 27-08-2009 CrysAlis171 .NET).

[78]. CRYSALISPRO, Oxford Diffraction Ltd., Version 1.171.33.46 (release 27-08-2009 CrysAlis171 .NET); Empirical absorption correction using spherical harmonics, implemented in SCALE3 ABSPACK scaling algorithm.

[79]. J. De Meulenaar and H. Tompa, *Acta Crystallogr., Sect. A*, 1965, **19**, 1014.

[80]. G. Cascarano, A. Altomare, C. Giacovazzo, A. Guagliardi, A. G. G. Moliterni, D. Siliqi, M. C. Burla, G. Polidori and M. Camalli, *Acta Crystallogr., Sect. A*, 1996, **52,** 79.

[81]. D. J. Watkin, C. K. Prout, J. R. Carruthers and P.W. Betteridge, *CRISTAL Issue 11*, Chemical Crystallography Laboratory, Oxford, UK, 1999.

[82]. R. I. Cooper, A. L. Thompson and D. J. Watkin, *J. Appl. Cryst.*, 2010, **43**, 110.

[83]. G.M. Sheldrick, *SHELXTL Version 2014/7, http://shelx.uni-ac.gwdg.de/SHELX/index.php*.

[84]. G. M. Sheldrick, *Acta. Cryst.*, 2015, **71**, 3.

[85]. P. McArdle, *J.Appl.Cryst.*, 1995, **28**, 65.

[86]. M. J. Frisch, G. W. Trucks, H. B. Schlegel, G. E. Scuseria, M. A. Robb, J. R. Cheeseman, G. Scalmani, V. Barone, G. A. Petersson, H. Nakatsuji, X. Li, M. Caricato, A. V. Marenich, J. Bloino, B. G. Janesko, R. Gomperts, B. Mennucci, H. P. Hratchian, J. V. Ortiz, A. F. Izmaylov, J. L.Sonnenberg, D. Williams-Young, F. Ding, F. Lipparini, F. Egidi, J. Goings, B. Peng, A. Petrone, T. Henderson, D. Ranasinghe, V. G. Zakrzewski, J. Gao, N. Rega, G. Zheng, W. Liang, M. Hada, M. Ehara, K. Toyota, R. Fukuda, J. Hasegawa, M. Ishida, T. Nakajima, Y. Honda, O. Kitao, H. Nakai, T. Vreven, K. Throssell, J. A. Montgomery, Jr., J. E. Peralta, F. Ogliaro, M. J. Bearpark, J. J. Heyd, E. N. Brothers, K. N. Kudin, V. N. Staroverov, T. A. Keith, R. Kobayashi, J. Normand, K. Raghavachari, A. P. Rendell, J. C. Burant, S. S. Iyengar, J. Tomasi, M. Cossi, J. M. Millam, M. Klene, C. Adamo, R. Cammi, J. W. Ochterski, R. L. Martin, K. Morokuma, O. Farkas, J. B. Foresman, and D. J. Fox, Gaussian, Inc., Wallingford CT, 2016.

[87]. D. Beck, *J. Chem. Phys.* 1993, **98**, 5648.

[88]. Lee, W. Yang, and R. G. Parr, *Phys. Rev. B: Condense Matter Mater. Phys.* 1988 **37**, 785.

[89]. M. A. Spackman and D. Jayatilaka, *Cryst. Eng. Comm.* 2009, **11**, 19-32.

[90]. J. J. McKinnon, D. Jayatilaka and M.A. Spackman, *Chem Commun.,* 2007, 3814.

[91]. J. J. Koenderink and A. J. Van Doorn, *Image and Vision Computing*, 1992, **10**, 557.

[92]. J. J. McKinnon, M.A. Spackman and A.S. Mitchel, *Acta Crys. B,* 2004, **60,** 627

[93]. M.A. Spackman and D. Jayatilaka, *Cryst Eng. Comm,* 2009, **11** , 19.